Acta Crystallographica Section D
Biological Crystallography
ISSN 0907-4449

Crystallization and preliminary X-ray diffraction analysis of pyranose 2-oxidase from the white-rot fungus *Trametes multicolor*

B. Martin Hallberg,[a]† Christian Leitner,[b] Dietmar Haltrich[b] and Christina Divne[a]*

[a]Department of Biotechnology, KTH, Albanova University Center, SE-106 91 Stockholm, Sweden, and [b]Institute of Food Technology, Division of Biochemical Engineering, BOKU–University of Natural Resources and Applied Life Sciences, Vienna, A-1190 Vienna, Austria

† Present address: Department of Biochemistry and Biophysics, Stockholm University, Albanova University Center, SE-106 91, Stockholm, Sweden.

Correspondence e-mail: divne@biotech.kth.se

Received 5 September 2003
Accepted 29 October 2003

Pyranose 2-oxidase (P2Ox) is a 270 kDa homotetrameric flavoenzyme that catalyzes the oxidation of D-glucose to 2-keto-D-glucose. P2Ox participates in lignin degradation by white-rot fungi and a tentative role of the enzyme is the production of H_2O_2 for lignin peroxidases. Crystals of *Trametes multicolor* P2Ox were grown from monomethylether PEG 2000, sodium acetate, $MgCl_2$ and Ta_6Br_{12}. They belong to space group $P2_1$, with unit-cell parameters a = 99.9, b = 101.7, c = 135.6 Å, β = 90.85°. X-ray diffraction data to 2.0 Å resolution were collected using synchrotron radiation. Self-rotation function calculations suggest that the asymmetric unit contains one homotetramer with 222 point-group symmetry.

1. Introduction

The fungal enzyme pyranose 2-oxidase (P2Ox; pyranose:oxygen 2-oxidoreductase; synonym glucose 2-oxidase; EC 1.1.3.10) is an intracellular homotetrameric enzyme located primarily in the hyphal periplasmic space, where it catalyzes the oxidation of D-glucose and other aldopyranoses at C-2 to the corresponding 2-ketoaldoses concomitantly with the reduction of O_2 to H_2O_2 (Janssen & Ruelius, 1968). The enzyme is widely distributed among wood-degrading basidiomycetes (Danneel *et al.*, 1992; Leitner *et al.*, 1998; Volc *et al.*, 1985) and has been suggested to provide H_2O_2 for lignin-degrading peroxidases (Daniel *et al.*, 1994; Volc *et al.*, 1996) or to have a role in the reduction of benzoquinones formed during ligninolysis (Leitner *et al.*, 2001). P2Ox has been purified at high yield from mycelial extracts of *Trametes multicolor* and it has been shown to be a functional homotetramer with a molecular weight of approximately 270 kDa and one covalently bound flavin adenine dinucleotide (FAD) cofactor per monomer (Leitner *et al.*, 2001). In northern Europe, this basidiomycete (synonym *T. ochracea*) contributes significantly to the degradation of hardwood, mainly *Betula* species. To date, mRNA sequences have been reported for P2Ox from *Trametes versicolor* (Nishimura *et al.*, 1996; sp:P79076), *Peniophora* sp. SG (tr:Q8J136), *Tricholoma matsutake* (tr:Q8J2V8), *Trametes hirsuta* (Patent No. US6146865; sp:59097) and *Trametes ochracea* (gb:AY291124).

There is no structural information available for any P2Ox. Detailed information about the structural determinants of the catalytic machinery of this enzyme is desirable for several reasons. P2Ox has been shown to have an important role in lignin degradation by white-rot fungi and, in addition, the enzyme can be used biotechnologically to produce a large number of rare sugars and fine chemicals, including compounds relevant to the medicine and food industries.

2. Material and methods

2.1. Protein preparation and crystallization

Intracellular *T. multicolor* strain MB49 P2Ox was purified from mycelial extracts as described previously (Leitner *et al.*, 2001). Single crystals were obtained at 293 K using the hanging-drop vapour-diffusion method (McPherson, 1982). The drops were prepared by mixing 1 µl of 5 mg ml^{-1} protein in 20 m*M* sodium acetate buffer pH 4.2 and 1 µl reservoir solution. Initial crystallization conditions were established using sparse-matrix screening (Jancarik & Kim, 1991) with Crystal Screen (Hampton Research, Riverside, CA, USA). Showers of thin yellow crystal plates (Fig. 1*a*) grew within 1 h from formulation No. 37 [0.1 *M* sodium acetate trihydrate pH 4.6, 8%(*w*/*v*) PEG 4000].

2.2. Optimization of crystallization conditions

The crystallization conditions were optimized by screening different types of PEG at different concentrations and screening for optimal pH in steps of 0.1 pH unit between pH 4.0 and 5.0. Optimized conditions were found with monomethylether (mme) PEG 2000 and pH 4.7. Additional optimization was performed with Additive Screen 1 (Hampton Research, Riverside, CA, USA) and positive results were obtained when $MgCl_2$ was added to the mother liquor to a final concentration of 0.1 *M*. Crystals suitable for X-ray diffraction

 DOI: 10.1107/S0907444903024922

experiments were grown from droplets prepared by mixing 1 µl of 5 mg ml^{-1} protein in 20 m*M* sodium acetate buffer pH 4.2 and 1 µl reservoir solution containing 10%(*w*/*v*) mme PEG 2000, 0.1 *M* $MgCl_2$ and 0.1 *M* sodium acetate buffer pH 4.7. The hanging drops were suspended over 0.4 ml reservoir solution in a Falcon 24-well multiplate and streak-seeded immediately after preparation. Yellow octahedral prisms of approximate dimensions 0.15 × 0.1 × 0.1 mm grew overnight (Fig. 1*b*). P2Ox crystals were also grown from identical droplets as above but with the addition of tantalum cluster (Ta_6Br_{12}) to a final concentration of 2 m*M* in the drop.

2.3. X-ray diffraction experiment

Prior to data collection, the crystal was mounted in a cryoloop and swept through cryoprotectant solution containing 25% glycerol, 10% PEG 400, 10%(*w*/*v*) mme PEG 2000, 0.1 *M* $MgCl_2$ and 0.1 *M* sodium acetate buffer pH 4.7 and flash-frozen in liquid nitrogen. X-ray diffraction were collected at the L_{III} absorption edge of Ta from a P2Ox crystal co-crystallized with Ta_6Br_{12} cluster at 100 K at the European Synchrotron Radiation Facility (Grenoble, France; beamline ID14-4, λ = 1.2552 Å). Bragg reflections to 1.8 Å resolution were recorded on a Q4R ADSC CCD detector. Data to 2.0 Å resolution were integrated with *MOSFLM* (Leslie, 1996) and reduced with *SCALA* (Evans, 1993) and *TRUNCATE* (French & Wilson, 1978) from the *CCP*4 suite of crystallographic programs (Collaborative Computational Project, Number 4, 1994). Data-collection statistics are summarized in Table 1.

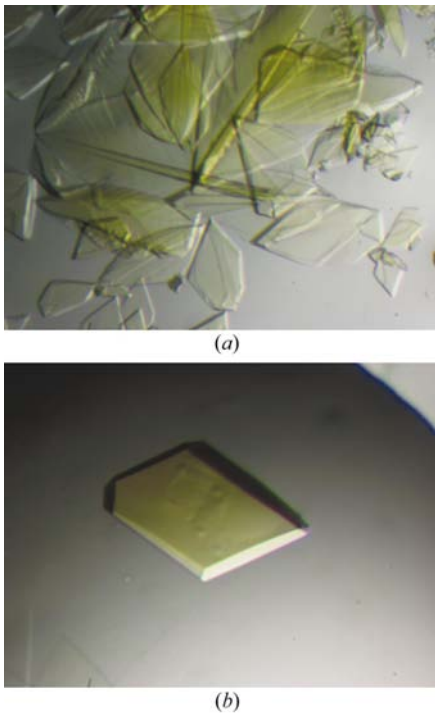

Figure 1
Yellow monoclinic crystal prisms of *T. multicolor* P2Ox (*a*) prior to and (*b*) after optimization.

2.4. Native Patterson function and self-rotation function calculations

Native Patterson function calculations were performed with diffraction data between 15 and 3.0 Å resolution using the fast Fourier transform as implemented in the *CCP*4 suite of crystallographic programs (Collaborative Computational Project, Number 4, 1994). Ordinary self-rotation function (RF) calculations were performed with *GLRF* (Tong & Rossmann, 1990, 1997) included in the *REPLACE* program package (Tong, 1993).

3. Results and discussion

3.1. Crystallization and X-ray diffraction analysis

Native P2Ox crystals typically diffract to a maximum resolution of 2.5 Å using synchrotron radiation (data not shown). Co-crystallization with tantalum cluster, however, yielded isomorphous crystals with increased diffraction power, *i.e.* to 1.8 Å resolution, compared with the native crystals (Table 1; Fig. 2). Ta-P2Ox crystals were primitive monoclinic with systematic absences for odd *k* indices (0*k*0, *k* = 2*n* + 1), consistent with $P2_1$ in the *b*-unique setting. The unit-cell parameters are *a* = 99.9, *b* = 101.7, *c* = 135.6 Å, β = 90.85°, giving a volume of the crystallographic unit cell of 13.8 × 10^5 Å^3. Considering that P2Ox is a functional homotetramer, the asymmetric unit is most probably occupied by one complete 270 kDa homotetramer, which would give a V_M value of 2.50 Å^3 Da^{-1} (Matthews, 1968), corresponding to a solvent content of 50%. Each P2Ox subunit contains roughly 620 amino acids (70 kDa), thus giving 2480 residues for one biologically functional tetrameric assembly per asymmetric unit.

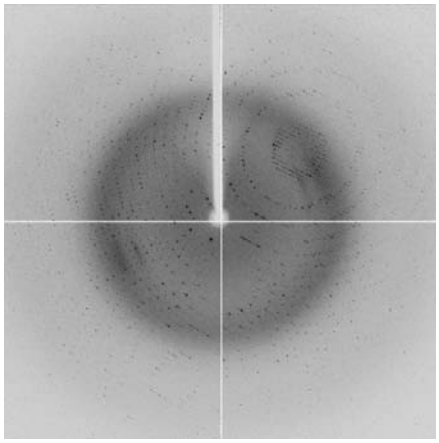

Figure 2
Representative diffraction image from the tantalum P2Ox data. The diffraction limits at the corners and edges of the detector are 1.6 and 2.0 Å resolution, respectively.

Table 1
Data-collection statistics.

Values in parentheses are for the highest resolution shell.

Resolution range (Å)	39.8–2.00 (2.11–2.00)
No. unique reflections	182655 (26344)
Completeness (%)	99.9 (99.9)
Multiplicity	3.7 (3.4)
R_{merge}† (%)	9.0 (19.1)
R_{meas}‡ (%)	12.8 (26.2)
$\langle I/\sigma(I)\rangle$§	5.4 (3.2)

† $R_{merge} = [\sum_{hkl}\sum_i |I - \langle I\rangle|/\sum_{hkl}\sum_i |I|] \times 100$. ‡ R_{meas} is the redundancy-independent merging *R* factor according to Diederichs & Karplus (1997). § As given by the program *SCALA* (Evans, 1993).

3.2. Non-crystallographic symmetry

Functional homotetramers typically obey either 222 (*D*2) or fourfold (*C*4) point-group symmetry. However, at least one example exists, *e.g.* the structure of peanut lectin (Banerjee *et al.*, 1994), in which the homotetramer obeys neither *D*2 nor *C*4 symmetry, but displays an 'open' quaternary structure. Since the asymmetric unit of the monoclinic

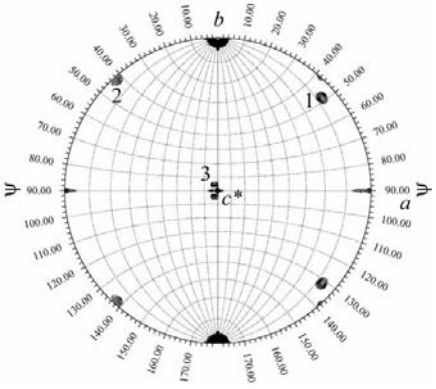

Figure 3
Stereographic projection of κ = 180° from an ordinary self-rotation function calculated in space group $P2_1$. The circumference of the circle corresponds to φ = 0°. Self-RF calculations were performed with the following parameters: slow RF mode; Patterson integration radius 35 Å; resolution range 20–4.0 Å; polar convention *XYK*; orthogonalization convention *AXABZ*. The plot was contoured between 0.5 and 4σ in increments of 0.1σ. The peak heights for the three twofold axes 1, 2 and 3 (see text) correspond to 28% (1), 27% (2) and 24% (3) of the origin peak, respectively. The signal-to-noise ratio is approximately 1.5 (*i.e.* the ratio between the weakest peak and the highest noise peak).

crystals is likely to contain one complete homotetramer, native Patterson function calculations and self-RF calculations were carried out in order to investigate the nature of the non-crystallographic symmetry (NCS) operators. The native Patterson function was devoid of significant peaks, thus confirming that the space group is indeed $P2_1$ and not $P2$ and that the P2Ox monomers must be related by rotational symmetry. The self-RF calculated with *GLRF* (Tong & Rossmann, 1990, 1997) revealed unambiguous peaks in the $\kappa = 180^\circ$ section (Fig. 3) and an essentially featureless $\kappa = 90^\circ$ section.

Besides the peak originating from the crystallographic 2_1 axis at $\varphi = 0$, $\psi = 0^\circ$, the $\kappa = 180^\circ$ section of the self-RF is dominated by three peaks at $\varphi = 7$, $\psi = 48^\circ$ (1), $\varphi = 179$, $\psi = 42^\circ$ (2) and $\varphi = 93$, $\psi = 85.5^\circ$ (3). These peaks correspond to three mutually orthogonal twofold rotation axes, indicating that the P2Ox homotetramer obeys 222 point-group symmetry. Axis 1 is positioned between the crystallographic *a* and *b* axes, rotated 48° from the *b* axis. Axis 2 lies perpendicular to axis 1 and is rotated 42° from the *b* axis, again between axes *a* and *b*. The third twofold rotation axis is orthogonal to the *a* and *b* axes and is within 5° of the crystallographic *c* axis.

3.3. Outlook for structure determination

The amino-acid sequence of *T. multicolor* P2Ox is known (gb:AY291124) and from sequence-similarity searches we can conclude that the identity within the P2Ox family is high. To other known protein sequences similarity is typically low, encompassing primarily the $\beta\alpha\beta$ mononucleotide-binding motif frequently encountered in nicotinamide- and flavin-dependent enzymes (Wierenga *et al.*, 1986). Interestingly, the fold-recognition server *3D-PSSM* (Kelley *et al.*, 2000) unambiguously places the P2Ox sequences in the GMC (glucose-methanol-choline) family of FAD-dependent oxidoreductases (Cavener, 1992), together with members such as *Aspergillus niger* glucose 1-oxidase, *Brevibacterium sterolicum* cholesterol oxidase and *Phanerochaete chrysosporium* cellobiose dehydrogenase flavoprotein domain (DH_{cdh}). Consequently, molecular-replacement (MR) calculations were initially considered. We have used various GMC oxidoreductase models as search probes for MR calculations, but without success. From our previous experience with GMC enzymes, small but distinct hinge-bending motions between the FAD-binding and substrate-binding domains (Hallberg *et al.*, 2002) are likely to hamper MR calculations.

The potential usefulness of the tantalum clusters for SIRAS and SAD phasing to low resolution has been analyzed, but no solutions have been found. Our current efforts are therefore focused on obtaining other heavy-atom derivatives for use in MIR(AS) and/or SAD/MAD experiments.

This study was supported by grants from Austrian Research Foundation (project No. FWF P15719) to DH and from the Swedish Research Council for Environment, Agricultural Sciences and Spatial Planning and the Swedish Research Council to CD.

References

Banerjee, R., Mande, S. C., Ganesh, V., Das, K., Dhanaraj, V., Mahanta, S. K., Suguna, K., Surolia, A. & Vijayan, M. (1994). *Proc. Natl Acad. Sci. USA*, **91**, 227–231.
Cavener, D. R. (1992). *J. Mol. Biol.* **223**, 811–814.
Collaborative Computational Project, Number 4 (1994). *Acta Cryst.* D**50**, 760–763.
Daniel, G. J., Volc, J. & Kubatova, E. (1994). *Appl. Environ. Microbiol.* **60**, 2524–2532.
Danneel, H.-J., Ullrich, M. & Giffhorn, F. (1992). *Enzyme Microb. Technol.* **14**, 898–903.
Diederichs, K. & Karplus, P. A. (1997). *Nature Struct. Biol.* **4**, 269–275.
Evans, P. R. (1993). *Proceedings of CCP4 Study Weekend. Data Collection and Processing*, edited by L. Sawyer, N. Isaacs & S. Bailey, pp. 114–122. Warrington: Daresbury Laboratory.
French, G. S. & Wilson, K. S. (1978). *Acta Cryst.* A**34**, 517–525.
Hallberg, B. M., Henriksson, G., Pettersson, G. & Divne, C. (2002). *J. Mol. Biol.* **315**, 421–434.
Jancarik, J. & Kim, S.-H. (1991). *J. Appl. Cryst.* **24**, 409–411.
Janssen, F. W. & Ruelius, H. W. (1968). *Biochim. Biophys. Acta*, **167**, 501–510.
Kelley, L. A., MacCallum, R. M. & Sternberg, M. J. E. (2000). *J. Mol. Biol.* **299**, 499–520.
Leitner, C., Haltrich, D., Nidetzky, B., Prillinger, H. & Kulbe, K. D. (1998). *Appl. Biochem. Biotechnol.* **70–72**, 237–248.
Leitner, C., Volc, J. & Haltrich, D. (2001). *Appl. Environ. Microbiol.* **67**, 3636–3644.
Leslie, A. G. W. (1996). *Jnt CCP4/ESF–EAMCB Newsl. Protein Crystallogr.* **32**, 7–8.
McPherson, A. (1982). *Preparation and Analysis of Protein Crystals.* New York: John Wiley & Sons.
Matthews, B. W. (1968). *J. Mol. Biol.* **33**, 491–497.
Nishimura, I., Okada, K. & Koyama, Y. (1996). *J. Biotechnol.* **52**, 11–20.
Tong, L. (1993). *J. Appl. Cryst.* **26**, 748–751.
Tong, L. & Rossmann, M. G. (1990). *Acta Cryst.* A**46**, 783–792.
Tong, L. & Rossmann, M. G. (1997). *Methods Enzymol.* **276**, 594–611.
Volc, J., Denisova, N. P., Nerud, F. & Musílek, V. (1985). *Folia Microbiol.* **30**, 141–147.
Volc, J., Kubatova, E., Daniel, G. & Prikrylova, V. (1996). *Arch. Microbiol.* **165**, 421–424.
Wierenga, R. K., Terpstra, P. & Hol, W. G. J. (1986). *J. Mol. Biol.* **187**, 101–107.